



Contents lists available at ScienceDirect

Earth and Planetary Science Letters

journal homepage: www.elsevier.com/locate/epsl

New GPS constraints on the kinematics of the Apennines subduction

Roberto Devoti ^a, Federica Riguzzi ^{a,b,*}, Marco Cuffaro ^{b,c}, Carlo Doglioni ^b^a Istituto Nazionale di Geofisica e Vulcanologia, sez. CNT, Roma, Italy^b Dipartimento di Scienze della Terra, Università La Sapienza, Roma, Italy^c IGAG-CNR, Roma, Italy

ARTICLE INFO

Article history:

Received 15 June 2007

Received in revised form 13 June 2008

Accepted 16 June 2008

Available online 28 June 2008

Editor: R.D. van der Hilst

Keywords:

GPS

ITRF2005

Adriatic

Eurasia

Africa

Euler poles

subduction hinge

subduction rate

Apennines

slab kinematics

ABSTRACT

We present the velocity field of the Italian area derived from continuous GPS observations from 2003 to 2007. The GPS sites were installed by different institutions and for different purposes; they cover the whole country with a mean inter-site distance of about 60 km and provide a valuable source of data to map the present day kinematics of the region.

The absolute ITRF2005 rotation poles and rates of Eurasia, Africa and Adriatic plates are estimated, to study the kinematics along their boundaries in the Apennines belt.

The Corsica–Sardinia block, coherently moving as the Eurasia plate, is used as reference of the upper plate for the Apennines subduction zone. We apply a simple kinematic model to estimate the rates and spatial pattern of the subduction along the Apennines. We identify at least four different, independently moving, lower plates, i.e., the Adriatic (diverging and internally segmented), Ionian, Sicily and Africa (converging) plates with different subduction rates. The conservative estimates of the subduction rate are ~5 mm/yr in the Calabrian Arc, ~1.5 mm/yr in Sicily, and ~0.9 mm/yr in the northern Apennines. This variegated mixture of behaviors seems to reflect the variable lithospheric thickness and composition of the lower plates inherited from the Mesozoic rifting. An unexpected along strike contraction is observed along the western side of the central-northern Apennines.

Velocities are estimated both relative to Eurasia, and relative to the deep and shallow hotspot reference frames (HSRF). The hotspot representation seems more coherent with the geophysical and geological constraints along the subduction system, in which the Adriatic and Ionian plates move SW-ward and their deeper slab portions provide an obstacle to the opposite relative mantle flow.

All these patterns better reconcile if the subduction process is conceived as a passive feature controlled by the far field plate velocities and the relative “eastward” mantle flow acting on a disrupted slab.

© 2008 Elsevier B.V. All rights reserved.

1. Introduction

In the general paradigm of plate tectonics, along a subduction zone the lower plate converges relative to the upper plate and penetrates the mantle. However, relative to a fixed point in the upper plate U , the lower plate L can converge, diverge or be stationary, and the subduction can be still active. The transient subduction hinge H can converge, diverge, or be stationary, and the subduction rate V_S is given by the velocity of the hinge H minus the velocity of the lower plate L , i.e., $V_S = V_H - V_L$ (Doglioni et al., 2006). Therefore the subduction rate is not equal to the convergence rate, which can be either positive or negative, and the subduction can occur even if the lower plate diverges or is stationary relative to the upper plate in case the subduction hinge migrates away from the upper plate faster than the lower plate. We

show here that the combination of lower plate and subduction hinge velocities relative to the assumed fixed upper plate can provide different kinematics even along a single subduction zone. The Apennines belt and related Tyrrhenian back-arc basin (Fig. 1) are taken as an example of subduction zone where these parameters vary along strike. Using a dense GPS network widespread along the study area (Fig. 2), we have analyzed and interpreted the different kinematics, comparing the results with geological studies. This study presents the current GPS velocity field in the Italian area obtained combining three different permanent GPS network solutions.

It will be shown that at least four different regimes can occur along the Apennines belt, since the subduction rate depends both on the convergence or divergence rate and the velocity of the subduction hinge that can either converge or diverge relative to the upper plate, decreasing or increasing the speed of the subduction respectively.

Along some segments, the subduction occurs even in spite of a lower plate diverging from the upper plate. The motion of the Apennines and the Adriatic deformed margins is also expressed in the deep and shallow HSRF.

* Corresponding author. Istituto Nazionale di Geofisica e Vulcanologia, sez. CNT, Roma, Italy.

E-mail address: riguzzi@ingv.it (F. Riguzzi).

2. Geodynamic setting: the Adriatic microplate and the Apennines subduction

The Apennines–Tyrrhenian system formed as accretionary prism (Bally et al., 1986) and back-arc basin respectively in the hangingwall of the Neogene to present arcuate W-directed subduction of the Adriatic continental and Ionian oceanic lithospheres (e.g. Doglioni et al., 1999; Panza et al., 2003; Faccenna et al., 2004). Moving along strike, the slab had and still has different behaviors, both in terms of seismicity (Pondrelli et al., 2004), surface geology and kinematics, due to the relevant anisotropies in thickness and composition of the downgoing lithosphere (Calcagnile and Panza, 1981; Carminati et al., 2005). The lower plate of the Apennines–Maghrebides subduction system is in fact composed of different types of lithosphere, inheriting pre-existing Mesozoic, Cenozoic and even active rifting episodes. An active rifting occurs in the Sicily channel (e.g. Corti et al., 2006), separating the Sicilian continental lithosphere from the main Africa plate (Fig. 1). Moving E-ward, the Malta escarpment is a right-lateral active transtensional system (Doglioni et al., 2001) re-using a pre-existing Mesozoic continent–ocean transition between Sicily and the Ionian deep basin (Catalano et al., 2001). The transition between the Ionian and the Adriatic continental lithosphere is the conjugate margin of the Malta escarpment. This margin should likely be considered active since plate kinematic models predict independent and different velocities of the Adriatic plate (e.g. Battaglia et al., 2004). The deformed margins of the Mesozoic Adriatic plate are inferred in Fig. 1. They are chiefly made

of passive continental margin sequences shortened by the Apenninic, Alpine and Dinaric subduction zones-related orogens. In the Alps the Adriatic plate overrode the Eurasia plate, whereas along the Apennines and Dinarides, the Adriatic lithosphere represents the footwall plate. Most of the Adriatic original lithosphere has disappeared along the Apennines and Dinarides subduction zones, possibly with oceanic crust at the leading edge. The Ionian (partly oceanic) lithosphere has a differential right-lateral retreat with respect to Sicily continental lithosphere. The latter is spreading apart with respect to Africa, generating the Sicily channel rift (Fig. 1).

The Adriatic plate underwent rifting episodes throughout the Mesozoic and became separated from the Africa plate with the opening of the Ionian basin, which age and nature are still matter of debate (Catalano et al., 2001). Since the Cretaceous, the Alpine subduction developed carrying the northern and western margins of the Adriatic plate over the Eurasia plate. Contemporaneously, the Adriatic plate subducted Eurasia toward NE-ward along the Dinarides. Since Oligocene times, the Adriatic plate inverted its behavior along its western margin, and switched from being the upper plate of the Alpine subduction, to the lower plate during the Apennines subduction (Doglioni et al., 1998). However within the Adriatic plate, different kinematic behaviors can be distinguished. For example, the Puglia foreland is uplifting (Doglioni et al., 1994), whereas the central-northern Adriatic Sea is subsiding as the Po Basin to the N (Doglioni, 1994). Practically all the Adriatic plate is subject to ongoing deformation; in fact the area unaffected by horizontal deformation (compression, strike-slip,

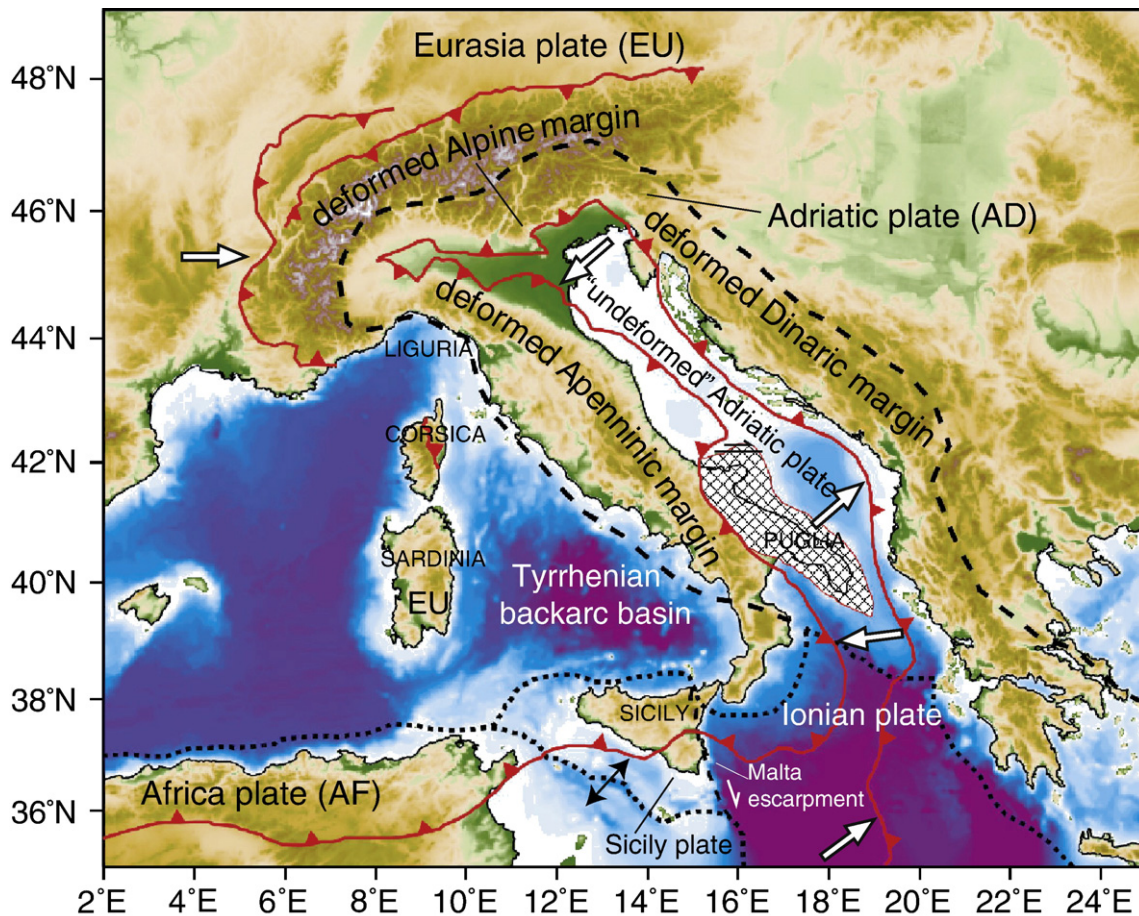


Fig. 1. Along the Apennines subduction, the footwall is composed by four plates, the Adriatic, Ionian, Sicilian and African lithospheres. The Adriatic microplate subducts underneath the Apennines and the Dinarides, whereas it overrides the European plate along the Alps. The Adriatic “undeformed” part (red line) is restricted in the central-northern part of the Adriatic Sea. Part of it is uplifted by a lithospheric buckling in the Puglia region (grid area), and the remaining part is mostly tilted by the Apennines foreland monocline, associated to the subduction hinge. The black dashed line delimiting the border of the continental part of the Adriatic microplate is inferred after some retrodeforming of its margins. A large part of the Adriatic original lithosphere has disappeared along the subduction zones bordering the plate. The Ionian (partly oceanic) lithosphere retreats right laterally with respect to the continental lithosphere of Sicily, which is in turn moving NE with respect to Africa, generating the rift in the Sicily channel.

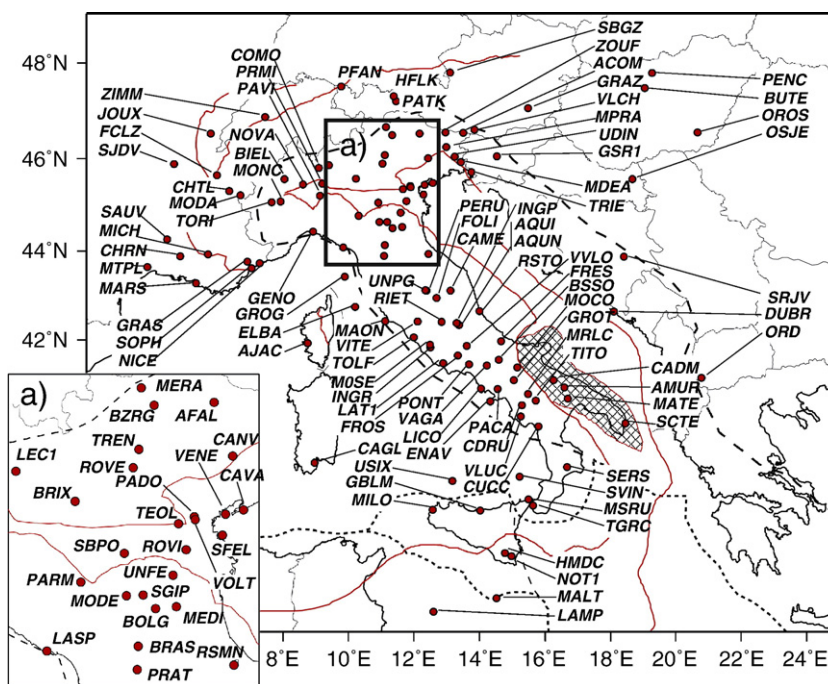


Fig. 2. The complete GPS network solution comes from the combination of three main sub-networks: the Italian network, composed of 102 permanent sites, 91 located in Italy and other 11 in the surrounding countries; the Austrian Reference Extended (ARE) network (Pany et al., 2001) and the REGAL network (Calais et al., 2000). Acronyms and red spots indicate GPS stations used in this study. Very few sites are located outside the deformational area. Moreover those few sites are located in the subsiding foreland area. Therefore there are no good kinematic constraints on the Adriatic microplate. (For interpretation of the references to color in this figure legend, the reader is referred to the web version of this article.)

ripping) is undergoing either tilting and subsidence (the whole Adriatic Sea and Po Basin) or uplift (Puglia). The different vertical behaviors can be ascribed to the Apennines slab retreat (subsidence) or lithospheric buckling (uplift). Therefore no GPS sites can be considered completely untouched by active deformation within the Adriatic plate (Fig. 2).

3. Velocity field of the Italian area

The complete GPS network solution arises from the combination of three main sub-networks (Fig. 2): the Italian network, composed of 102 permanent sites, 91 located in Italy and other 11 in the surrounding countries; the Austrian Reference Extended (ARE) network (Pany et al., 2001) and the REGAL network (Calais et al., 2000).

We implement a rigorous combination strategy based on the complete covariance matrices and a convenient handling of constraints, as described in Davies and Blewitt (2000). The combination of independent solutions provides a valuable means to compare coordinate and velocity solutions at common sites, and to minimize the systematic errors associated with each individual processing strategy (e.g. Nocquet and Calais, 2004).

3.1. Italian area network

At present, the permanent GPS sites installed in the Italian area together with the historical late-nineties permanent sites constitute a dense network covering the whole country with a mean inter-site distance of about 60 km. A total of 102 sites were considered including a few located in the surrounding area. The network is formed by stations owned by different agencies and authorities, primarily by the INGV Integrated National GPS Network (RING, Selvaggi et al., 2006), the Italian GPS Fiducial Network (IGFN, Vespe et al., 2000), the European EUREF network (Bruyninx, 2004), and minor clusters owned by regional authorities and universities. We selected a limited time span, from DOY 1/2003 to DOY 54/2007 because most of the GPS sites were installed in the last few years. The velocity uncertainties of each

site have been evaluated in detail using the error analysis technique developed by Williams (2003).

We processed the GPS phase data in six regional clusters, each containing at least 11 common anchor sites, i.e. selected sites based on station performance and geographical distribution, used as core sites for the reference frame definition and the cluster combination. We have analyzed the daily RINEX files with the Bernese Processing Engine v.5.0 (Beutler et al., 2007) applying the quasi-ionosphere-free (QIF) strategy for the ambiguity resolution and constraining each daily solution to the coordinates of MATE (Matera) to 0.01 mm (apriori sigma). Subsequently, each solution has been unconstrained (Davies and Blewitt, 2000) removing the apriori constraints and adding loose translation and scale constraints, then the loosely constrained cluster solutions of each day have been merged into daily loosely constrained solutions (Bianco et al., 2003). In order to express the velocity field in a coherent reference frame, we adopt the official ITRF2005 (International Terrestrial Reference Frame), recently released by the International Earth Rotation and Reference Systems Service (Altamimi et al., 2007). The daily combined network solutions were rigidly transformed into the ITRF2005 frame estimating translations and scale parameters. There are 13 core sites contributing to the rigid transformation and globally the weighted RMS of the residuals after the transformation is about 2–3 mm. The official ITRF2005 solution contains embedded offsets for each site data history, i.e. different sets of coordinates and velocities are provided for different time spans; nevertheless we choose a set of fiducial sites whose velocities are at any time constant over the entire period.

3.2. ARE network

The daily solutions of various GPS networks in the Eastern Europe area are available at the Observatory Lustbuehel (OLG, Graz). We considered the Austrian Reference Extended solutions (ARE) that contain some Austrian reference sites and also the permanent sites from the Central European Geodynamic Research Project (CERGOP).

The daily solutions are available in SINEX (Solution INdependent EXchange) format containing coordinate estimates and covariance matrices. They were obtained with different versions of the processing software and with sporadic changes in the analysis procedures through the years. The time interval considered in our analysis span from DOY 221/1998 until DOY 365/2006.

We recognize differences in the daily solutions, the majority of them (until DOY 287/2006) tightly constrained to a single site (0.01 mm apriori sigma), the remaining solutions loosely constrained (about 4 m apriori sigma). To properly set the reference frame, all the daily solutions were unconstrained, removing the apriori covariance, adding minimal constraints and subsequently rigidly transformed into the ITRF2005 reference solution. Due to the limited extension of the network a simple translation and scale Helmert transformation was applied. A maximum number of 23 anchor sites contribute to the Helmert transformation through the time series, but occasionally outliers were isolated and edited from the transformation itself, thus on the average, 10–13 sites did actually contribute. For the anchor sites, the global weighted RMS of the coordinate residuals after the transformation was only slightly higher (3–4 mm) than for the Italian network.

3.3. The REGAL network

We used the available velocity solution of the permanent GPS network on the western Alps (Calais et al., 2000). The solution file contains loosely constrained site velocity and coordinates obtained from daily coordinate solutions (from DOY 001/1996 to DOY 200/2003) processed by Nocquet and Calais (2004) with the GAMIT-GLOBK

software (King and Bock, 2002; Herring et al., 1990). The overall network consists of 58 sites, 27 of them being strictly REGAL sites whereas the others are spread all over the Western Europe. The apriori constraints are 10 m for the coordinates and 1 m/yr for the velocities.

Since the daily solutions were not available, the coordinate/velocity solution has been aligned to the ITRF2005 reference frame through a 14 parameter Helmert transformation after applying the corresponding 14 inner constraints to the covariance matrix. Seven anchor sites contribute to the transformation yielding a global weighted RMS of residuals of a few mm in the coordinates and a few tenths of mm/yr in the velocities.

3.4. Time series analysis

Since the two available time series (Italian and ARE networks) differ substantially in terms of repeatability and spectral content, we prefer to estimate the velocity fields separately and to combine the two velocity fields thereafter. Thus all the daily solutions were stacked separately into normal equation matrices and site positions and velocities were estimated simultaneously along with annual signals and sporadic offsets at epochs of instrumental changes. The estimated parameters will depend on the whole covariance matrices and we note that the covariances between sites are effective in tightening up weakly constrained velocities, e.g. when the time series is very short or badly conditioned. As a result we could observe a rather good spatial coherence in the velocity field also for those sites that nominally should suffer from high systematic errors due to their short observation period. In a few sites we judge the horizontal

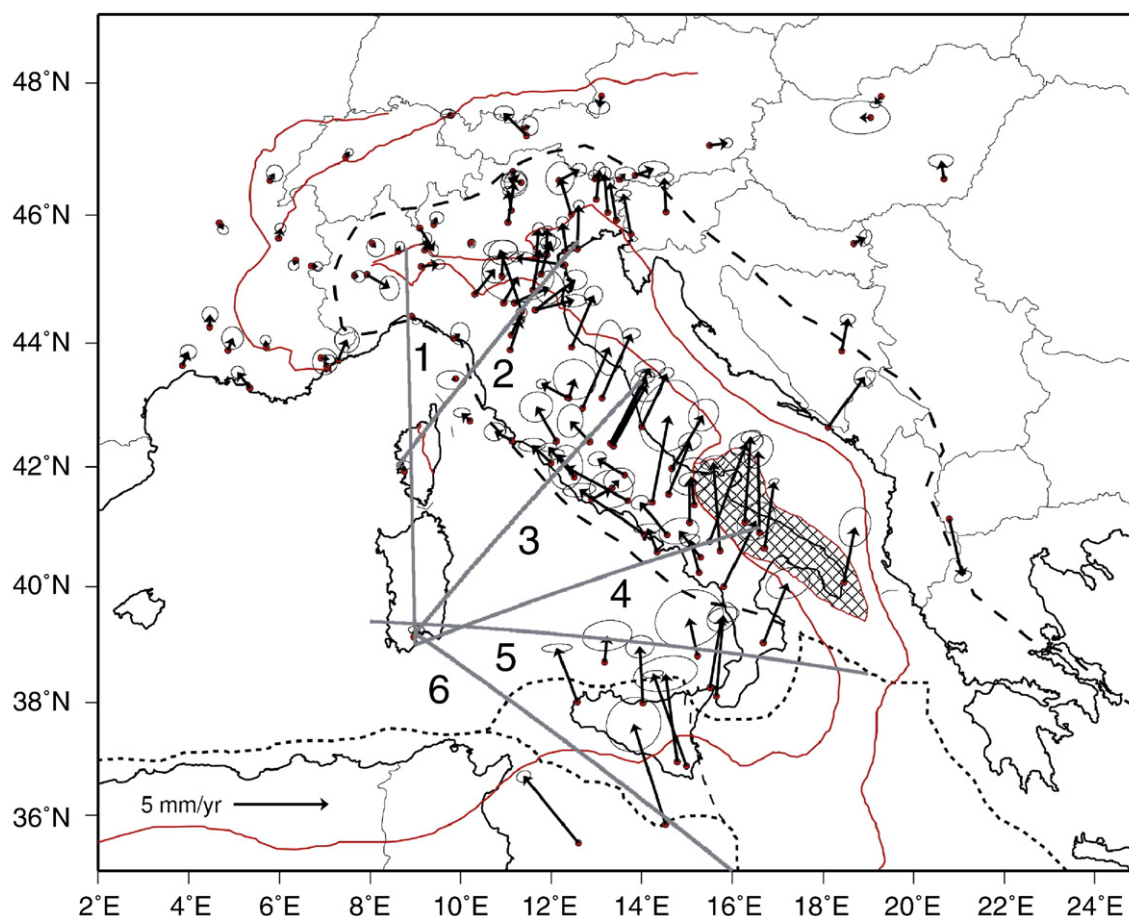


Fig. 3. GPS velocities with respect to Eurasia and rescaled ellipses at 68% probability level. Confidence ellipses include the variance of the rotation vector defining the reference frame estimated in ITRF2005. Grey lines are the sections (1–6) along which velocities and uncertainties at 68% probability level are projected (Fig. 7). Note the relevant change in direction between the sites located in the western central and southern Apennines with respect to the eastern side, providing evidence for a major tectonic change and transtensional rift along that boundary.

velocities acceptable even if derived from time series as short as 1.5 years. Concerning the vertical motion, since the intrinsic repeatability of the vertical component is a factor of 2–4 worse than the horizontal component, we found that the four-year period is not sufficient for a reliable estimation and most vertical movements do not exceed the noise. The whole velocity field of the Italian area is shown in Fig. 3 with respect to the Eurasian reference frame, the ellipses being the 2 degrees of freedom, 68% confidence region.

3.5. Error analysis

The formal standard deviations associated with the velocity estimates are known to be underestimated, depending on the deviation from normality of the detrended residuals. For independent randomly distributed residuals, the formal error decreases as $1/\sqrt{n}$ where n is the number of daily solutions. A number of studies have demonstrated that the GPS time series show significant temporal correlations that must be taken into account to get reliable estimates of the velocity uncertainties (Williams et al., 2004; Mao et al., 1999; Johnson and Agnew, 1995, and references therein). In particular, the spectral content of geodetic time series is dominated by white noise at high frequencies and a rising power density at low frequencies. We scaled the formal errors of the GPS rates using the approach developed in Williams (2003), accounting for a power-law noise and a constant white noise term estimated directly from the detrended residuals. We estimate three parameters (the spectral index κ , white noise and colored noise amplitudes) for each time series component after subtracting a linear trend and an annual sinusoid. The three-parameter model characterizes the noise content of each GPS site,

allowing the spectral index to range continuously from a pure white noise ($\kappa=0$), through flicker noise ($\kappa=-1$) up to a random walk ($\kappa=-2$) noise. Thus, the estimates allow scaling the formal errors associated to each site velocity in proportion to the noise amplitudes and length of the time series. We obtained scale factors spread between the tenth and ninetieth percentiles of 3.2 and 9.7, with a median value of 5.7. Generally, the vertical rate component presents a slightly higher scale factor (median 6.5) than the planar component (median 5.2). In the east and north components the estimated spectral index ranges between $\kappa=-0.2$ and $\kappa=-0.9$ (average -0.60) with an average spectral amplitude of $1.2 \text{ mm/yr}^{-\kappa/4}$, thus being halfway between white noise and flicker noise. The Median Time $T_{1 \text{ mm/yr}}$ for the velocity uncertainty to reach 1 mm/yr, relevant for the detection of changes in velocity, is on average 0.5 yr, very close to other findings (Williams et al., 2004; Beavan, 2005).

To test the consistency of the scaled errors with the velocity repeatability, we have evaluated the mutual velocity differences at overlapping sites. A total of 30 independent site velocity differences can be formed and their residuals could be useful to test the reference system realization. The overall WRMS of the velocity residuals are 0.4 and 3.6 mm/yr (horizontal and vertical) and the medians of the scaled uncertainty are 0.6 and 2.5 mm/yr (horizontal and vertical). The normalized χ^2 (per degree of freedom) is $\chi^2_v=1.62$ which has to be compared with the higher value of $\chi^2_v=16.5$, obtained without scaling the velocity errors. Since the systematic differences (rotation–translation and scaling of the velocity fields) are not statistically significant, we conclude that the scaled velocity errors are consistent with the velocity repeatability.

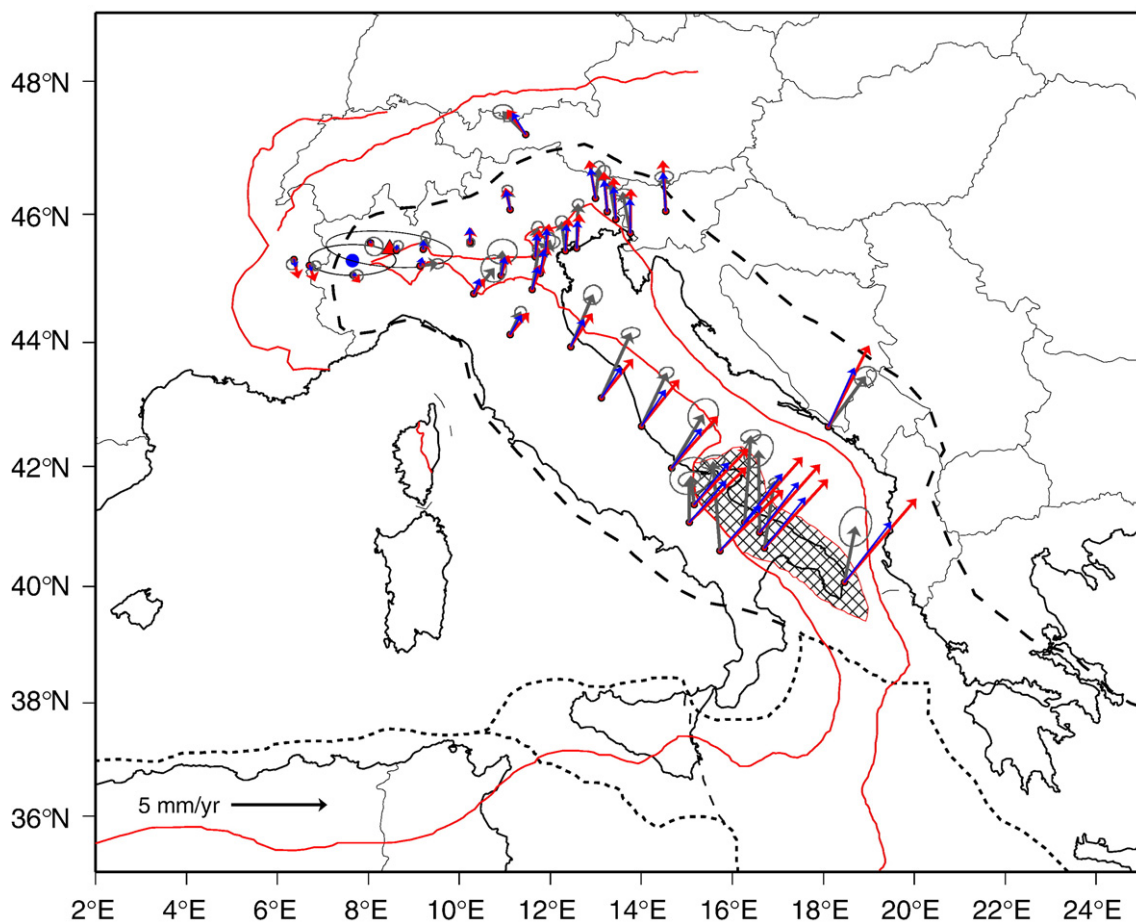


Fig. 4. Comparison among AD1 (blue vectors) and AD2 (red vectors) solutions for the Adriatic microplate motion with respect to Eurasia, GPS velocities are in grey.

4. Africa–Eurasia convergence

We estimate the plate rigid motion directly from the official ITRF2005 velocity solution. The rigid plate motion is statistically inferred using a simple χ^2 test-statistics to select the coherent subset of sites defining a stable plate, as suggested in [Nocquet et al. \(2001\)](#). Starting from three central European sites (pilot triad: WSRT, WZSR and ZIMM) a total of 24 sites result assigned to a stable plate with $\chi^2_{\nu} = 1.46$. The absolute ITRF2005 Eurasia pole and rotation rate are 55.85°N , 95.72°W and $0.266 \pm 0.003^\circ/\text{Myr}$, consistent with previous ITRF2000 and recent ITRF2005 poles ([Fernandes et al., 2003](#); [Kremer et al., 2003](#); [D'Agostino and Selvaggi, 2004](#); [Serpelloni et al., 2005](#); [Altamimi et al., 2007](#)). A few central European sites, including POTS, BOR1, LAMA and JOZE, are surprisingly rejected both at 95% and 99% significance level. We argue that the associated errors are probably underestimated, i.e. too small if compared to their velocity residuals and should be recalibrated in successive ITRF realization. Furthermore all the Siberian sites are systematically rejected from being rigidly connected with the central Europe region. In particular, all the sites located east of ARTU (58°E) have a 2–3 mm/yr W-ward residual velocity pattern that cannot be accommodated by a variance rescaling.

The ITRF2005 Africa Euler pole is estimated using the same χ^2 test procedure, starting from a triad located west of the East African Rift (MAS1, Goug and HRAO); the final selection is composed by 10 sites. The relatively high misfit ($\chi^2_{\nu} = 4.76$) suggests that the associated ITRF2005 variances could be underestimated by the same χ^2_{ν} factor, or the rigid plate model is inadequate for these sites. Scaling the ITRF2005 velocity variances by the same factor leads to a substantially equivalent Euler pole, accepting a total of 10 sites belonging to the African plate. Thus we conclude that the pole is rather stable nevertheless the declared ITRF2005 variances are probably underestimated by the same factor. The estimated absolute pole and rotation rate are 49.40°N , 83.06°W and $0.268 \pm 0.003^\circ/\text{Myr}$, consistent at 1-sigma level with the recent ITRF2005 value ([Altamimi et al., 2007](#)).

Our relative Africa–Eurasia pole agrees in the Mediterranean area within 0.5 ± 0.1 mm/yr with respect to recent estimates ([D'Agostino and Selvaggi, 2004](#); [Nocquet and Calais, 2004](#); [Reilinger et al., 2006](#); [Serpelloni et al., 2007](#); [Altamimi et al., 2007](#)), very close to the repeatability observed between the different solutions. Thus the convergence velocity in the Mediterranean region is relatively insensitive to the selection and time span of stations used to estimate the rotation vector.

5. The Adriatic microplate kinematics

The existence of an Adriatic microplate lying at the margin of Eurasian and African plates has been under discussion for years, considering both the assumption of an independent microplate ([Ward, 1994](#)), and proposing the Adriatic area as a promontory of the African plate ([Channell, 1996](#)). Global scale plate kinematic models, such as NUVEL1-A ([DeMets et al., 1994](#)), based on geological and geophysical data, or REVEL ([Sella et al., 2002](#)), based on recent space geodesy data, did not include the Adriatic plate motion, but they substantially presented different estimated velocities of the major plates (i.e. Eurasia and Africa) at this common boundary. The Adriatic microplate motion has been recently interpreted as the combination of two blocks (i.e., north Adriatic and south Adriatic) with independent kinematics ([Battaglia et al., 2004](#)) or as the relative motions of two blocks attached to the major plates ([Oldow et al., 2002](#)). These different interpretations arise from the fact that the Adriatic boundaries are not completely known and the Adriatic motion is only weakly constrained; in fact this microplate is generally not taken into account in global plate datasets (e.g. [Bird, 2003](#)).

The Adriatic deformation zones involve a major part of the Italian peninsula and most of the Italian GPS stations lie inside the deformed

Appenninic and Alpine margins of the Adriatic microplate boundaries ([Fig. 1](#)).

Exploiting our new GPS velocity field, we attempt to estimate different Euler poles of the Adriatic microplate using the blind χ^2 test mentioned before. Our best model (AD1) results from the pilot triad (PADO, ROVI, VENE) and supplies a set of 13 consistent sites located both inside and outside the undeformed part of Adriatic plate. The normalized post-fit is rather good ($\chi^2_{\nu} = 1.72$) and the pole parameters are reasonably uncorrelated, revealing a coherent rigid plate motion. With respect to Eurasia, the AD1 pole and rotation rate are 45.29°N , 7.65°E and $0.216 \pm 0.023^\circ/\text{Myr}$. The χ^2 test rejects systematically all the sites located inside the deformed area S of 44°N ([Fig. 4](#)) producing a significant misfit in the south Adriatic region (AMUR, CADM, DUBR, MATE, SCTE), where lithospheric buckling is active ([Doglioni et al., 1994](#)). These sites move to the N instead of NNE predicted from AD1 motion ([Fig. 4](#)). On the other hand, the consistency of these sites in defining a separate south Adriatic block is poor and leads to a bad-conditioned pole estimate. In alternative, considering the entire Adriatic block as a whole (AD1 plus south Adriatic sites) the fit gets even worse ($\chi^2_{\nu} = 17.08$), the relative pole shifts to west (44.34°N , 3.78°E) and the rate halves to $0.123 \pm 0.030^\circ/\text{Myr}$.

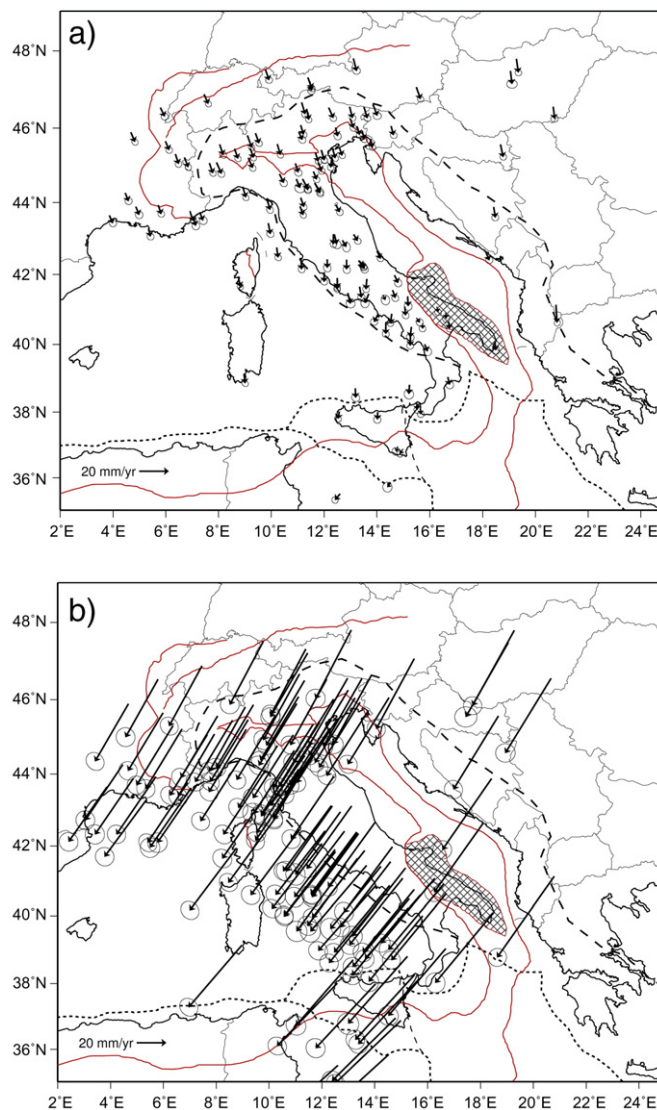


Fig. 5. Velocities in the deep (a) and shallow (b) hotspot reference frames of [Crespi et al. \(2007\)](#).

A further model (AD2) is instead computed selecting eight GPS stations located in the Po basin, within the red line of Fig. 1, the less deformed part of the Adriatic plate (exception is SFEL, probable outlier). In this case the estimates present a higher misfit ($\chi^2=6.98$) with respect to AD1; the relative pole is near AD1 (45.45°N, 8.57°E) but the rotation rate is much higher (0.327 ± 0.103)/Myr (Fig. 4). Although the rotation rates are different (AD1 about 1.6 times AD2), the high uncertainty of the AD2 estimate prevents a reliable distinction from AD1. The high variability observed between different pole realizations is similar to what observed by other authors (Battaglia et al., 2004; Grenerczy et al., 2005), precluding the eventual interpretation of the whole Adriatic region moving as a rigid plate. Neither the more elaborate block model seems to be able to adequately represent the complexity of the Adriatic kinematics (Battaglia et al., 2004). The weakness of the Adriatic pole estimates seems to originate from the particular site placement, restricted in a small region where different geodynamic settings coexist. Most of the sites defining AD1 are located in presently active areas deformed either by the Apennines (BRAS, TORI), Alps (CHTL, MODA, PATK, NOVA, TREN), Dinarides (MDEA) or the subsiding foredeep of the Apennines (VENE, PADO, SBPO and ROVI), as shown in Figs. 1 and 2. The sites located in the eastern side of the central-northern Apennines show a gradual decrease in velocity moving NW-ward. This slowing down has generally been interpreted as related to the rotation of the Adriatic microplate with a pole located in NW Italy. However, the sites are all located in the allocthonous hangingwall of the Apennines subduction zone, which is NE-ward retreating along its northern arm. A number of independent evidences indicate that the depth of the slab, the back-arc spreading, the arc volcanism, the seismicity and the shortening in the accretionary prism decrease moving from the central to the northwestern Apennines. Therefore, the apparent coherence found when estimating poles is not necessarily related to the rotation of the Adriatic lower plate, but could be attributed to the variation of the Adriatic slab retreat rate relative to the upper European plate, decreasing from SE to NW along the Apennine belt (Doglioni, 1991). Under this hypothesis, any Adriatic pole estimate results weak and rather unconstrained if a comprehensive slab retreat model is not considered.

6. Motion relative to the mantle

We compute the motion of the Italian area relative to the HSRF (Fig. 5), introducing the net-rotation angular velocity to switch from the No-Net-Rotation frame (ITRF2005) to the HSRF (Jurdy, 1990; Cuffaro and Jurdy, 2006). In particular, we transform the ITRF2005 velocities into the deep and shallow HSRF (Crespi et al., 2007; Cuffaro and Doglioni, 2007), assuming a lithospheric net-rotation angular velocity computed by Crespi et al. (2007). In the deep HSRF the motion of Adriatic area is very low, while in the shallow HSRF it is SW-ward at about 5 cm/yr. The shallow hotspot velocity field seems to be more coherent with geological constraints along the subduction system, in which the Adriatic and Ionian microplates move SW-ward and their deeper slab portions provide an obstacle to the opposite relative mantle flow.

Shear wave splitting analysis shows seismic anisotropy W–E directed in most of the Tyrrhenian Sea, becoming parallel to the subduction strike along the Apennines (e.g. Baccheschi et al., 2007). This is consistent with a W to E mantle flow that is kinematically required by the E-ward slab retreat, regardless it is the cause or the consequence of the rollback (Doglioni et al., 1999). Since the Adriatic slab sinks even if the lower plate is diverging relative to the upper plate, it confirms how the retreat is related to the interplay between slab and the hosting mantle, i.e., slab pull or E-ward mantle flow. However, most of the subducted Adriatic plate beneath the Apennines can be inferred as continental on the basis of the passive continental margin sediments accreted in the accretionary prism. Continental lithosphere is by definition lighter than the underlying mantle, questioning the role of the slab-pull.

7. Basic kinematics along a subduction in the upper plate reference frame

In order to describe the details of the kinematics across the Apennine belt, we wish to recall first some simple concepts on the subduction kinematics (Doglioni et al., 2006).

Let us consider a reference frame with three points, one attached to the upper plate (U), a second attached to the lower plate (L), and the third on the transient subduction hinge (H), as in Fig. 6. The point located on the upper plate is taken as fixed, i.e. its velocity is $V_U=0$ by definition. The motion of the two remaining points is considered relative to the fixed upper plate; in this frame, V_L is the velocity of the lower plate and V_H is the velocity of the hinge. If L and/or H move towards the fixed point U, then their velocities are assumed to be negative. If the L and/or H diverge from the upper plate, then V_H and V_L are positive.

Particular attention will be given to the effects of the kinematics of lower plate and hinge on the subduction velocity V_S . This is defined as the lithosphere entering the subduction zone per unit time and can be calculated simply by $V_S=V_H-V_L$ (Doglioni et al., 2006). V_L is easily derived from plate motion models. The exact determination of the hinge location is not easy due to the wideness of the rounded area characterized by dip changes from the horizontal lower plate lithosphere to the inclined downgoing slab. In general, the location of the hinge zone has been assumed to be close or coincident with that of the subduction trench (e.g. Heuret and Lallemand, 2005). However, the amount of accretion, i.e., the mass transfer from the lower to the upper plate, increases the volume of rocks in the hangingwall of the slab, partly inhibiting the back-arc spreading. Asthenospheric intrusion at the subduction hinge can also decrease the space for the back-arc spreading. Moreover, the extension in the hangingwall of the subduction hinge also contributes to render difficult the inference of the exact location of the subduction hinge from surface observations.

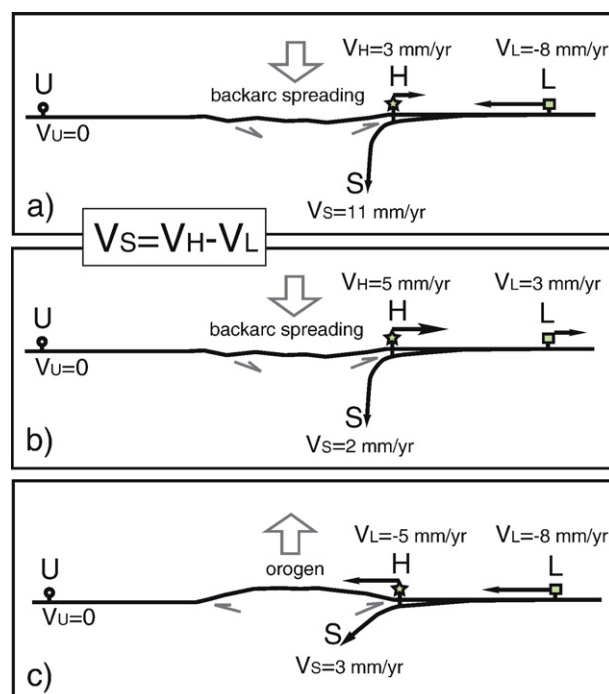


Fig. 6. Basic kinematics of subduction zones, assuming fixed the upper plate U. The lower plate is L, and the transient subduction hinge, H. The movements diverging from the upper plate are positive, whereas they are negative when converging. The subduction rate is $V_S=V_H-V_L$. Values are only as an example. The case a) has H diverging and L converging, whereas in b) also L is diverging. In these settings, a low prism and back-arc spreading form and they are more typical of W-directed subduction zones. In case c) L and H converge to form a double verging more elevated orogen (modified after Doglioni et al., 2006).

As explained in detail in [Doglioni et al. \(2007\)](#), due to the complexity of defining an accurate determination of H , the value of V_H is possibly underestimated, so that V_S has to be considered only as a minimum estimate of the subduction rate.

In order to show that different kinematic and tectonic settings coexist along a single subduction zone, with the aim of quantifying even as minimum estimates the different subduction rates of the Adriatic plate, we have analyzed the motions of selected, mostly Italian, GPS stations located on upper and lower plates and on the accretionary prism along sections through the Apennines.

8. Variable rates along the Apennines subduction

The horizontal GPS velocities are projected along some representative sections ([Figs. 7, 8, 10](#)) in order to highlight the different velocity trends across and along the Apenninic belt and to compare the components of V_H and V_L perpendicular to the trench ([Figs. 9, 10](#)).

From this paper and other analyses ([Devoti et al., 2002; Oldow et al., 2002; Hollenstein et al., 2003; Battaglia et al., 2004; Serpelloni et al., 2005](#)), the Corsica–Sardinia block (represented by CAGL and AJAC) displays a motion consistent with Eurasia. This block is considered a remnant of the upper plate boudinage in the back-arc

setting of the Apennines subduction ([Gueguen et al., 1997](#)). Therefore Corsica–Sardinia can be chosen as the upper plate of the subduction system and both CAGL and AJAC can be considered representative of U to select sections perpendicular to the Apennine chain ([Fig. 3](#)).

In [Fig. 7](#), the extensional and compressional regimes with respect to Eurasia are differentiated respectively by white and grey half spaces.

Due to the sparse order distribution of the GPS sites and the presence of Adriatic Sea, section 2 is the only one entirely crossing the Apenninic belt, and ending toward the Venice area, considered part of the stable foreland in the Adriatic lower plate. The extension smoothly starts at LASP station, near the eastern margin of the Tyrrhenian Sea ([Fig. 2](#)), reaching a maximum of about 2 mm/yr. In sections 3 and 4, crossing the Tyrrhenian Sea and the central and southern Apennines, the transition is steeper and the extension reaches its maximum value, about 3–4 mm/yr.

Exceptions to the extensional behavior are section 1, where neither extension nor compression is prevalent, and section 4, site ENAV, located in the Neapolitan volcanic area. In section 5 the paucity of GPS sites and the geographical shape of the Calabria region ([Fig. 3](#)) prevent a robust kinematic definition; however a low extension rate of about 1 mm/yr is identified across the southern Tyrrhenian Sea. Conversely,

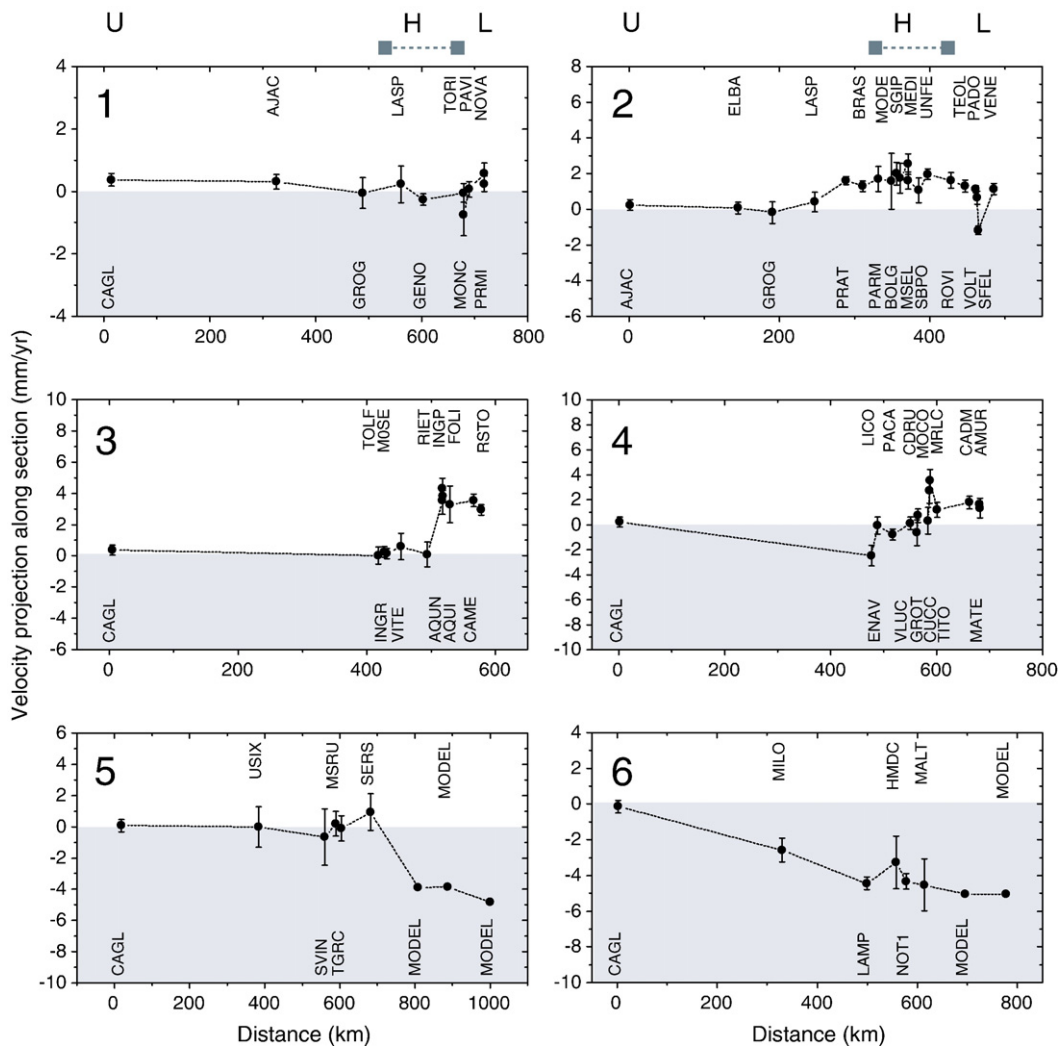


Fig. 7. Residual velocity components with respect to Eurasia and uncertainties at 68% probability, plotted as a function of distance along the sections of [Fig. 3](#). Grey and white indicate respectively the areas of convergence and extension with respect to the upper plate U ($V_U=0$), defined by the Eurasian frame, Corsica (AJAC)–Sardinia (CAGL). H, subduction hinge (the grey bar indicates uncertainty of its location), and L, lower plate. In sections 5 and 6, with MODEL are indicated hypothetical African sites whose velocities are computed from our Africa–Eurasia rotation vector.

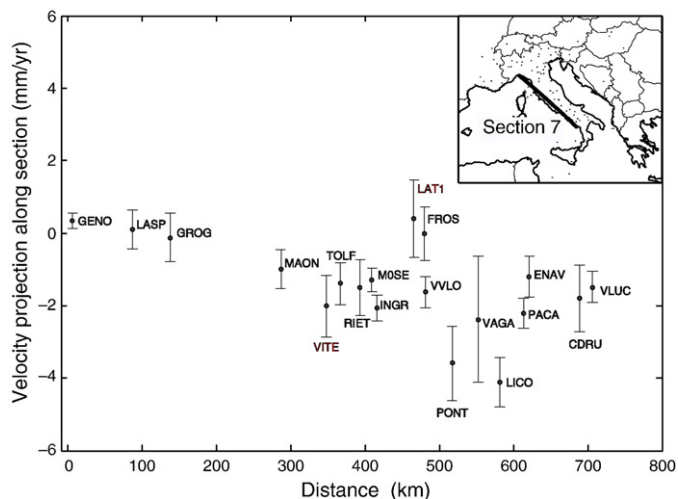


Fig. 8. Residual velocities with respect to Eurasia. Along the Tyrrhenian side of the belt an unexpected along strike compression is visible, with the southern sites moving NW-ward faster than the northern sites.

section 6 displays an unambiguous convergence trend. In these last two sections are shown hypothetical African sites whose velocities are computed by our Africa–Eurasia rotation vector. As expected, all these African sites lie well below the zero line, in the convergence grey area.

The increased density of GPS sites along the western Tyrrhenian Apennines strike allows evidencing a rather well defined pattern of NW-directed residual velocities, showing a compression component from SE to NW (Fig. 8). In the Calabrian arc the transition between the NW and the NE velocity directions occurs at about 40°N (Fig. 3) and corresponds to the paleomagnetic declination variations evident in Pleistocene sediments (Sagnotti and Meloni, 1993). It is unclear yet the cause of this compression component able to produce a mean velocity variation from about 2.4 to 0 mm/yr along this section. In our opinion

it is not possible to simply hypothesize a residual component of the Africa–Eurasia convergence, rather a coupling between lithosphere and mantle circulation around the slab (Montuori et al., 2007; Baccheschi et al., 2007). Alternatively, it could represent part of the dissipation of the Africa–Eurasia relative motion, or an unidentified tectonic deformation associated to the counterclockwise rotation in the western Apennines back-arc setting.

We further analyzed the Apennine belt using six cross-sections (Fig. 9) on which we projected the velocity component relative to CAGL or AJAC. These sections highlight five different geodynamic settings.

From Corsica to Liguria and south Piemonte in the northern Apennines, there is no significant relative motion: H, L and U have consistent motion within the errors (Fig. 10a), although GENO might not correctly represent the subduction hinge, being located in the stretched Alps. Moving from the Corsica–Sardinia block to NE, through Emilia and Veneto regions, the site of UNFE, assumed to be fairly representative of the subduction hinge, is moving away from the upper plate faster than sites located more to NE in the foreland, like VENE, so that $V_H > V_L$ (Fig. 10b). Ongoing extension documented in the central-northern Apennines (Hunstad et al., 2003) is consistent with the positive value of V_H (i.e., the hinge migrates toward the foreland), that explains the active spreading of the Tyrrhenian back-arc basin. The same geodynamic setting is evidenced in Fig. 10c.

In southern Apennines the setting changes (Roure et al., 1991), suggesting a slower velocity of the diverging hinge with respect to the foreland, i.e., both H and L move away from the upper plate, but the lower plate L seems faster. In this setting the slab is paradoxically moving away with respect the upper plate and subduction would result negative, Fig. 10d. This is compatible with the paucity of geological and geophysical data supporting active compression at the southern Apennines front, while active extension is widespread in the belt (Scrocca et al., 2005).

In a cross-section from Sardinia to Calabria and Ionian basin, the setting changes again (Fig. 10e). In this case, the Ionian (L) is

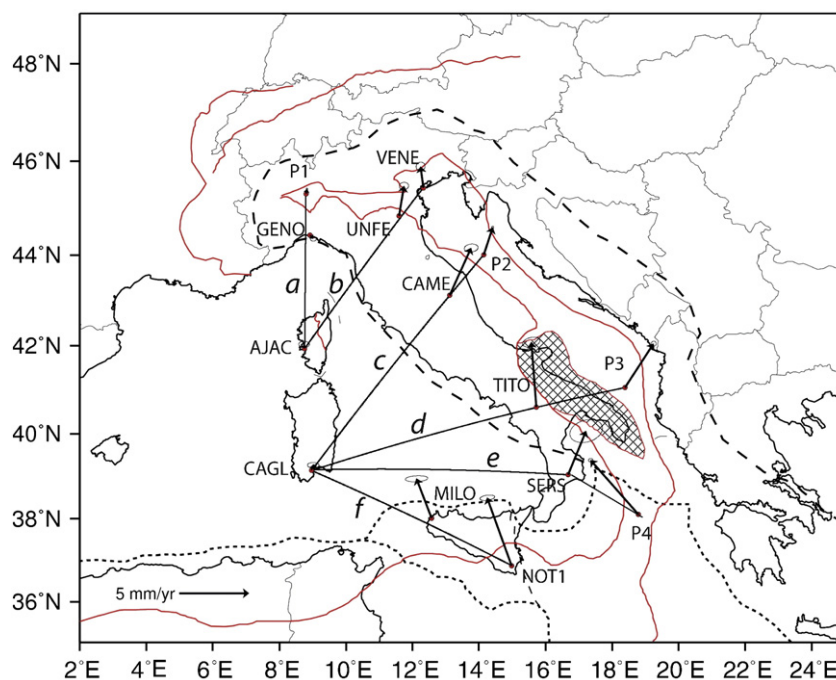


Fig. 9. Selected sections across the Apenninic arc: the sites of Cagliari (CAGL) and Ajaccio (AJAC), which are on the Sardinia–Corsica continental boudin, are considered part of Eurasia. GENO, Genova; UNFE, Ferrara; VENE, Venice; CAME, Camerino; TITO, Tito; SERS, Sersale; MILO, Trapani; NOT1, Noto; P1–2–3–4 velocities are computed from the Africa–Eurasia rotation vector, Adriatic (AD1) and Africa (AF) plate motions with respect to Eurasia (EU).

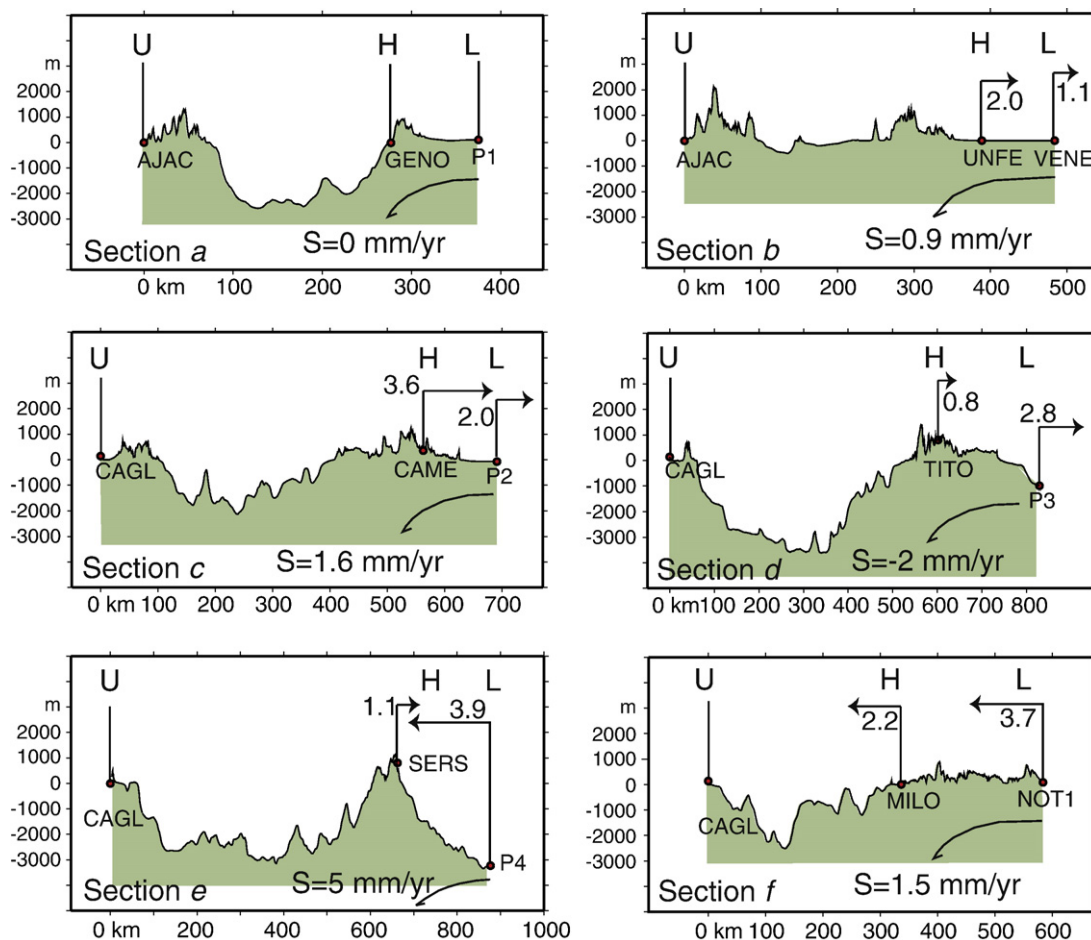


Fig. 10. Topographic profiles along the sections shown in Fig. 9. Along the Apenninic arc different relationships between U, H and L occur. The upper plate U is considered fixed (Sardinia–Corsica, CAGL and AJAC). The inferred subduction rates (S) are minimum estimates, as explained in Doglioni et al. (2007). Note that each section has different geodynamic settings and variable subduction rates. The rates of H and the lower plate L, projected on the sections, are in mm/yr. Section a) shows no significant relative motion and hence yields a zero subduction rate. Both sections b) and c) have H diverging from U faster than L. Section d) has the subduction rate paradoxically negative, pointing for a detachment of the slab but from the surface. The fastest subduction rate is along the Calabrian arc (section e) where H diverges and L converges. Section f) rather shows L converging faster than H.

converging relative to U. During present times, it is doubtful if and how fast Calabria (H) is still moving E-ward relative to Sardinia (U), in the frame of still active extension of the Tyrrhenian (Goes et al., 2004; Pondrelli et al., 2004; D'Agostino and Selvaggi, 2004). Anyway our GPS data seem to support a still active extension at a rate of about 1.1 mm/yr (Fig. 10e). On the other hand, both seismicity and seismic reflection profiles suggest active, although slow, extension in the Tyrrhenian Sea (Scrocca et al., 2003; Doglioni et al., 2004; Pondrelli et al., 2004; Chiarabba et al., 2005). An increase of accretion in the Ionian prism of the Apennines should provide an upper plate crustal thickening and widening, partly preventing back-arc extension. Along this section we observe the fastest subduction rate (Fig. 10e) with a minimum value of about 5.0 ± 2.2 mm/yr.

From Sardinia to Sicily, and from Sicily foreland to S, the Africa velocities (V_L) are oriented towards CAGL, but in northern Sicily (H) the movement is slower than in the foreland to S. In this setting (Fig. 10f), H is approaching U, with a slower velocity than the lower plate L, i.e., $|V_L| > |V_H|$. This is consistent with the compressive seismicity both south and north of Sicily (Chiarabba et al., 2005). The back-arc area along this section is then shrinking.

However, in the southern Tyrrhenian Sea, different settings may coexist in a single area due to the 3D nature of the subduction. For example, in northern Sicily, convergence of the hinge relative to the

upper plate in a NW–SE section concurs with an E–W extension related to the divergence of the hinge in Calabria. Therefore compressive–transpressive tectonic features overlap with extensional–transtensional faults in the southern Tyrrhenian Sea. This is consistent with seismic section interpretation and seismicity of the area (Chiarabba et al., 2005; Jenny et al., 2006; Montuori et al., 2007).

9. Discussion and conclusions

The updated GPS velocity field of the Italian area shown in this paper gives a detailed view of the motion around the Apennines, an accretionary wedge formed in the hangingwall of a W-directed subduction zone. The Apennines slab is composed by at least four different lithospheric segments with variable thickness, composition and velocity (the Adriatic, Ionian, Sicily and Africa domains). Each segment behaves differently in terms of tectonic setting and subduction rate. Extension appears more concentrated across the Apennines belt, whereas compression is evident along most of the eastern side. An unexpected along strike SE–NW compression is detected along the Tyrrhenian side of the western Apennines. Moreover the different azimuth and length of the vectors from the sites located in the western side with respect to the eastern side of the central and southern Apennines point for a narrow right-lateral

transensional boundary separating the two areas. Any attempt to estimate a rigid Adriatic pole results in a weak and rather unconstrained estimate. Consequently, we suggest that the variable Adriatic slab retreat rate could play an important role in the kinematic setting of the region.

In the Sicilian segment, the Tyrrhenian margin is undergoing a NNW-SSE-directed compression along the lithospheric heterogeneity (the transition between continental Sicily and the southern Tyrrhenian oceanic crust), while extension is contemporaneously operating along the E–W direction. Slow extension rate (at mm/yr level) is detected in the Tyrrhenian back-arc basin. A decrease or even a stop of the rifting in the Tyrrhenian Sea (in spite of normal fault-related seismicity (Pondrelli et al., 2004) has been proposed as related to the end of the slab rollback (D'Agostino and Selvaggi, 2004), although active convergence is documented between the Ionian Sea and the upper plate (e.g. Sardinia). As an alternative explanation, an increase of mass transfer from the lower to the upper plate in both areas has been proposed (Doglioni et al., 2007). Normal faulting in the prism may further enlarge the upper plate close to the subduction hinge, inhibiting the widening and measuring of the back-arc spreading. Nevertheless an extensional component is still visible (Fig. 10e).

The Apennines are an example denoting variable rates of subduction and different interplay between the behavior of H and L relative to U. The subduction rate is decreased or increased as a function of whether the subduction hinge converges or diverges relative to the upper plate, plus the convergence or divergence rate of the lower plate. The five main settings are 1) almost null motion of H and L (Fig. 10a, Liguria); 2) H diverges faster than L relative to U (Fig. 10b and c, northern and central Apennines); 3) H diverges slower than L (Fig. 10d, Puglia); 4) H diverges and L converges (Fig. 10e, Calabria); 5) H converges slower than L (Fig. 10f, Sicily). The transition between the different geodynamic settings can be either gradual (e.g. from section a to c), or along restricted transfer zones (e.g. between sections: c–d, Tremiti alignment; d–e, Apulian escarpment and e–f, Malta escarpment). The subduction rate is generally positive and ranges between 0 and 5 mm/yr from northern Apennines to the Calabrian arc; V_S is negative (Fig. 10d) when the lower plate diverges faster than the hinge. This kinematic setting seems a paradox but might represent the final evolution of the subduction zone.

At this stage we can infer some general considerations: 1) Variable geodynamic settings may coexist along a single subduction system (Fig. 10); 2) The subduction rate V_S is not equal to the convergence rate, but it is rather given by the relation $V_S = V_H - V_L$ (Fig. 6); 3) Subduction can occur even if the lower plate L diverges from the upper plate, if H moves away faster than L (Fig. 10); 4) In some areas, as in the southern Tyrrhenian sea, the 3D geometry of the back-arc spreading enables the coexistence of different geodynamic settings, e.g., NW–SE compression and E–W extension are co-working in the same area. The presence of different geodynamic settings supports a passive nature of these plate boundaries, which can rather be controlled by the far field plate velocity and the slab–mantle interaction, e.g. the relative E-ward mantle flow detected at a global scale in the HSRF (Crespi et al., 2007).

Acknowledgments

The manuscript was highly improved after the constructive comments of Robert King. We are grateful to all the persons working on GPS permanent networks and data bank maintenance (EUREF, REGAL, ARE, RING and many Italian institutions, universities and agencies). Special thanks are due to Grazia Pietrantonio. Discussions with Daniele Bernoulli, Eugenio Carminati and Davide Scrocca were very much appreciated. Giovanni Bortoluzzi, Marco Ligi and Valentina Ferrante are warmly thanked for helping with figure optimization. Many of the figures are made with the Generic Mapping Tools (Wessel and Smith, 1995).

Appendix A. Supplementary data

Supplementary data associated with this article can be found, in the online version, at doi:10.1016/j.epsl.2008.06.031.

References

- Altamimi, Z., Collilieux, X., Legrand, J., Garayt, B., Boucher, C., 2007. ITRF2005: a new release of the International Terrestrial Reference Frame based on time series of station positions and Earth Orientation Parameters. *J. Geophys. Res.* 112, B09401. doi:10.1029/2007JB004949.
- Baccheschi, P., Margheriti, L., Steckler, M.S., 2007. Seismic anisotropy reveals focused mantle flow around the Calabrian slab (southern Italy). *Geophys. Res. Lett.* 34, L05302. doi:10.1029/2006GL028899.
- Bally, A.W., Burbi, L., Cooper, C., Ghelardoni, R., 1986. Balanced sections and seismic reflection profiles across the central Apennine. *Mem. Soc. Geol. Ital.* 35, 257–310.
- Battaglia, M., Murray, M.H., Serpelloni, E., Bürgmann, R., 2004. The Adriatic region: an independent microplate within the Africa–Eurasia collision zone. *Geophys. Res. Lett.* 31, L09605. doi:10.1029/2004GL019723.
- Beavan, J., 2005. Noise properties of continuous GPS data from concrete pillar geodetic monuments in New Zealand and comparison with data from U.S. deep drilled braced monuments. *J. Geophys. Res.* 110. doi:10.1029/2005JB003642.
- Beutler, G., et al., 2007. Bernese GPS Software. In: Dach, R., Hugentobler, U., Fridez, P., Meindl, M. (Eds.), *Astronomical Institute, University of Bern* (January).
- Bianco, G., Devoti, R., Luceri, V., 2003. Combination of loosely constrained solutions. *IERS Tech. Note* (30), 107–109.
- Bird, P., 2003. An updated digital model of plate boundaries. *Geochem. Geophys. Geosyst.* 4 (3), 1027. doi:10.1029/2001GC000252.
- Bruyninx, C., 2004. The EUREF Permanent Network: a multi-disciplinary network serving surveyors as well as scientists. *Geoinformatics* 7, 32–35.
- Calais, E., Bayer, R., Chery, J., Cotton, F., Doerflinger, E., Flouzat, M., Jouanne, F., Kasser, M., Laplanche, M., Maillard, D., Martinod, J., Mathieu, F., Nicolon, P., Nocquet, J.-M., Scotti, O., Serrurier, L., Tardy, M., Vigny, C., 2000. REGAL: a permanent GPS network in the Western Alps. Configuration and first results. *C. R. Acad. Sci. Paris* 331, 435–442.
- Calcagnile, G., Panza, G.F., 1981. The main characteristics of the lithosphere–asthenosphere system in Italy and surrounding regions. *Pure Appl. Geophys.* 119, 865–879.
- Carminati, E., Negredo, A.M., Valera, J.L., Doglioni, C., 2005. Subduction-related intermediate-depth and deep seismicity in Italy: insights from thermal and rheological modeling. *Phys. Earth Planet. Int.* 149, 65–79.
- Catalano, R., Doglioni, C., Merlini, S., 2001. On the Mesozoic Ionian basin. *Geophys. J. Int.* 144, 49–64.
- Channell, J.E.T., 1996. Paleomagnetism and paleogeography of Adria, in paleomagnetism and tectonics of the Mediterranean Region. In: Morris, A., Tarling, D.H. (Eds.), *Geol. Soc. Spec. Publ.*, vol. 105, pp. 119–132.
- Chiarabba, C., Jovane, L., DiStefano, R., 2005. A new view of Italian seismicity using 20 years of instrumental recordings. *Tectonophysics* 395, 251–268.
- Corti, G., Cuffaro, M., Doglioni, C., Innocenti, F., Manetti, P., 2006. Coexisting geodynamic processes in the Sicily Channel. In: Dilek, Y., Pavlides, S. (Eds.), *Postcollisional Tectonics and Magmatism in the Mediterranean region and Asia*. *Geol. Soc. Am. Sp. Paper*, vol. 409, pp. 83–96.
- Crespi, M., Cuffaro, M., Doglioni, C., Giannone, F., Riguzzi, F., 2007. Space geodesy validation of the global lithospheric flow. *Geophys. J. Int.* 168 (2), 491–506.
- Cuffaro, M., Jurdy, D.M., 2006. Microplate motions in the hotspot reference frame. *Terra Nova* 18, 276–281.
- Cuffaro, M., Doglioni, C., 2007. Global kinematics in the deep vs. shallow hotspot reference frames. In: Foulger, G.R., Jurdy, D.M. (Eds.), *Plates, Plumes, and Planetary Processes*. *Geol. Soc. Am. Spec. Pap.*, vol. 430, pp. 359–374. doi:10.1130/2007.2430(18).
- Davies, P., Blewitt, G., 2000. Methodology for global geodetic timeseries estimation: a new tool for geodynamics. *J. Geophys. Res.* 105 (B5), 11083–11100.
- D'Agostino, N., Selvaggi, G., 2004. Crustal motion along the Eurasia–Nubia plate boundary in the Calabrian Arc and Sicily and active extension in the Messina Straits from GPS measurements. *J. Geophys. Res.* 109, B11402. doi:10.1029/2004JB002998.
- DeMets, C., Gordon, R.G., Argus, D.F., Stein, S., 1994. Effect of recent revisions to the geomagnetic reversal time scale on estimates of current plate motions. *Geophys. Res. Lett.* 21 (20), 2191–2194.
- Devoti, R., Ferraro, C., Gueguen, E., Lanotte, R., Luceri, V., Nardi, A., Pacione, R., Rutigliano, P., Sciarretta, C., Vespe, F., 2002. Geodetic control on recent tectonic movements in the central Mediterranean area. *Tectonophysics* 346, 151–167.
- Doglioni, C., 1991. A proposal of kinematic modelling for W-dipping subductions – possible applications to the Tyrrhenian–Apennines system. *Terra Nova* 3 (4), 423–434.
- Doglioni, C., 1994. Foredeeps versus subduction zones. *Geology* 22 (3), 271–274.
- Doglioni, C., Mongelli, F., Pieri, P., 1994. The Puglia uplift (SE-Italy): an anomaly in the foreland of the Apenninic subduction due to buckling of a thick continental lithosphere. *Tectonics* 13 (5), 1309–1321.
- Doglioni, C., Mongelli, F., Piali, G.P., 1998. Boudinage of the Alpine belt in the Apenninic back-arc. *Mem. Soc. Geol. Ital.* 52, 457–468.
- Doglioni, C., Gueguen, E., Harabaglia, P., Mongelli, F., 1999. On the origin of W-directed subduction zones and applications to the western Mediterranean. *Geol. Soc. London Sp. Publ.* 156, 541–561.
- Doglioni, C., Innocenti, F., Mariotti, S., 2001. Why Mt. Etna? *Terra Nova* 13 (1), 25–31.
- Doglioni, C., Innocenti, F., Morellato, C., Procaccianti, D., Scrocca, D., 2004. On the Tyrrhenian sea opening. *Mem. Descrittive Carta Geologica d'Italia* 64, 147–164.
- Doglioni, C., Carminati, E., Cuffaro, M., 2006. Simple kinematics of subduction zones. *Int. Geol. Rev.* 48, 479–493.

- Dogliani, C., Carminati, E., Cuffaro, M., Scrocca, D., 2007. Subduction kinematics and dynamic constraints. *Earth Sci. Rev.* 83, 125–175. doi:10.1016/j.earscirev.2007.04.001.
- Faccenna, C., Piromallo, C., Crespo-Blanc, A., Jolivet, L., Rossetti, F., 2004. Lateral slab deformation and the origin of the western Mediterranean arcs. *Tectonics* 23, TC1012. doi:10.1029/2002TC001488.
- Fernandes, R.M.S., Ambrosius, B.A.C., Noomen, R., Bastos, L., Wortel, M.J.R., Spakman, W., Govers, R., 2003. The relative motion between Africa and Eurasia as derived from ITRF2000 and GPS data. *Geophys. Res. Lett.* 30 (16), 1828.
- Goes, S., Giardini, D., Jenny, S., Hollenstein, C., Kahle, H.-G., Geiger, A., 2004. A recent tectonic reorganization in the south-central Mediterranean. *Earth Planet. Sci. Lett.* 226, 335–345.
- Grenerczy, G., Sella, G., Stein, S., Kenyeres, A., 2005. Tectonic implications of the GPS velocity field in the northern Adriatic region. *Geophys. Res. Lett.* 32, L16311. doi:10.1029/2005GL022947.
- Gueguen, E., Dogliani, C., Fernandez, M., 1997. Lithospheric boudinage in the Western Mediterranean back-arc basins. *Terra Nova* 9 (4), 184–187.
- Herring, T.A., Davis, J.L., Shapiro, I.I., 1990. Geodesy by radio interferometry: the application of Kalman filtering to the analysis of very long baseline interferometry data. *J. Geophys. Res.* 95 (B8), 12561–12581.
- Heuret, A., Lallemand, S., 2005. Plate motions, slab dynamics and back-arc deformation. *Phys. Earth Planet. Int.* 149, 31–51.
- Hollenstein, Ch., Kahle, H.-G., Geiger, A., Jenny, S., Goes, S., Giardini, D., 2003. New GPS constraints on the Africa–Eurasia plate boundary zone in southern Italy. *Geophys. Res. Lett.* 30 (18), 1935. doi:10.1029/2003GL017554.
- Hunstad, I., Selvaggi, G., D'Agostino, N., England, P., Clarke, P., Pierozzi, M., 2003. Geodetic strain in peninsular Italy between 1875 and 2001. *Geophys. Res. Lett.* 30 (4), 1181. doi:10.1029/2002GL016447.
- Jenny, S., Goes, S., Giardini, D., Kahle, H.-G., 2006. Seismic potential of Southern Italy. *Tectonophysics* 415, 81–101.
- Johnson, H.O., Agnew, D.C., 1995. Monument motion and measurements of crustal velocities. *Geophys. Res. Lett.* 22 (21), 2905–2908.
- Jurdy, D.M., 1990. Reference frames for plate tectonic and uncertainties. *Tectonophysics* 182, 373–382.
- King, R.W., Bock, Y., 2002. Documentation for the GAMIT analysis software, release 10.1. Massachusetts Institute of Technology, Cambridge, MA.
- Kreemer, C., Holt, W.E., Haines, A.J., 2003. An integrated global model of present-day plate motions and plate boundary deformation. *Geophys. J. Int.* 154, 8–34.
- Mao, A., Harrison, C.G.A., Dixon, T.H., 1999. Noise in GPS coordinate time series. *J. Geophys. Res.* 104 (B2), 2797–2816.
- Montuori, C., Cimini, G.B., Favali, P., 2007. Teleseismic tomography of the southern Tyrrhenian subduction zone: new results from seafloor and land recordings. *J.G. Res.* 112. doi:10.1029/2005JB004114.
- Nocquet, J.-M., Calais, E., 2004. Geodetic measurements of crustal deformation in the Western Mediterranean and Europe. *Pure Appl. Geophys.* 161.
- Nocquet, J.-M., Calais, E., Altamimi, Z., Sillard, P., Boucher, C., 2001. Intraplate deformation in western Europe deduced from an analysis of the International Terrestrial Reference Frame 1997 (ITRF97) velocity field. *J. Geophys. Res.* 106 (B6), 11,239–11,257.
- Oldow, J.S., Ferranti, L., Lewis, D.S., Campbell, J.K., D'Argenio, B., Catalano, R., Pappone, G., Carmignani, L., Conti, P., Aiken, C., 2002. Active fragmentation of Adria, the north Africa promontory, central Mediterranean orogen. *Geology* 30, 779–782.
- Pany, T., Pesec, P., Stangl, G., 2001. Network monitoring at the OLG analysis centre, Euref Symposium 2001. available at http://www.epncb.oma.be/_newsmails/papers/.
- Panza, G.F., Pontevivo, A., Chimera, G., Raykova, R., Aoudia, A., 2003. The lithosphere–asthenosphere: Italy and surroundings. *Episodes* 26 (3), 169–174.
- Pondrelli, S., Piromallo, C., Serpelloni, E., 2004. Convergence vs. retreat in Southern Tyrrhenian Sea: insights from kinematics. *Geophys. Res. Lett.* 31, L06611. doi:10.1029/2003GL019223.
- Reilinger, R., McClusky, S., Vernant, P., Lawrence, S., Ergintav, S., Cakmak, R., Ozener, H., Kadirov, F., Guliev, I., Stepanyan, R., Nadariya, M., Hahubia, G., Mahmoud, S., Sakr, K., ArRajehi, A., Paradissis, D., Al-Aydrus, A., Prilepin, M., Guseva, T., Evren, E., Dmitrova, A., Filikov, S.V., Gomez, F., Al-Ghazzi, R., Karam, G., 2006. GPS constraints on continental deformation in the Africa–Arabia–Eurasia continental collision zone and implications for the dynamics of plate interactions. *J. Geophys. Res.* 111 (B05411). doi:10.1029/2005JB004051.
- Roure, F., Casero, P., Vially, R., 1991. Growth processes and melange formation in the southern Apennines accretionary wedge. *Earth Planet. Sci. Lett.* 102, 395–412.
- Sagnotti, L., Meloni, A., 1993. Pleistocene rotations and strain in southern Italy: the example of the Sant'Arcangelo basin. *Annali di Geofisica* 36 (2), 83–95.
- Scrocca, D., Dogliani, C., Innocenti, F., Manetti, P., Mazzotti, A., Bertelli, L., Burbi, L., D'Offizi, S., 2003. CROP Atlas: seismic reflection profiles of the Italian crust. *Mem. Descrittive Carta Geologica d'Italia* 62, 194.
- Scrocca, D., Carminati, E., Dogliani, C., 2005. Deep structure of the Southern Apennines (Italy): thin-skinned or thick-skinned? *Tectonics* 24. doi:10.1029/2004TC001634.
- Sella, G.F., Dixon, T.H., Mao, A., 2002. REVEL: a model for recent plate velocity from space geodesy. *J. Geophys. Res.* 107 (B4), 2081. doi:10.1029/2000JB000033.
- Selvaggi, G., RING working group, 2006. La Rete Integrata Nazionale GPS (RING) dell'INGV: una infrastruttura aperta per la ricerca scientifica, X Conferenza nazionale dell'ASITA, Bolzano (Italy) 14–17 November.
- Serpelloni, E., Anzidei, M., Baldi, P., Casula, G., Galvani, A., 2005. Crustal velocity and strain-rate fields in Italy and surrounding regions: new results from the analysis of permanent and non-permanent GPS networks. *Geophys. J. Int.* 161 (3), 861–880. doi:10.1111/j.1365-246X.2005.02618.x.
- Serpelloni, E., Vannucci, G., Pondrelli, S., Argnani, A., Casula, G., Anzidei, M., Baldi, P., Gasperini, P., 2007. Kinematics of the Western Africa–Eurasia plate boundary from focal mechanisms and GPS data. *Geophys. J. Int.* 169 (3), 1180–1200. doi:10.1111/j.1365-246X.2007.03367.x.
- Vespe, F., Bianco, G., Fermi, M., Ferraro, C., Nardi, A., Sciarretta, C., 2000. The Italian GPS Fiducial Network: services and products. *J. Geodyn.* 30, 327–336.
- Ward, S., 1994. Constraints on the seismotectonics of the central Mediterranean from very long baseline interferometry. *Geophys. J. Int.* 11, 441–452.
- Wessel, P., Smith, W.H.F., 1995. New version of the Generic Mapping Tools (GMT) version 3.0 released. *Eos Trans. AGU* 76, 329.
- Williams, S.D.P., 2003. The effect of coloured noise on the uncertainties of rates estimated from geodetic time series. *J. Geod.* 76, 483–494.
- Williams, S.D.P., Bock, Y., Fang, P., Jamason, P., Nikolaidis, R.M., Prawirodirdjo, L., Miller, M., Johnson, D.J., 2004. Error analysis of continuous GPS position time series. *J. Geophys. Res.* 109. doi:10.1029/2003JB002741.